Novel sensor for sequential detection of copper and lactic acid

Vivek Shinh Kshtriya[a],Deepak Kumar Pandey[c],Sumit Kharbanda[d],Bharti Koshti[a], Chandra Kanth P[e],Dheeraj K Singh[c]*,Dhiraj Bhatia[d]*, Nidhi Gour[a, b]*

[a] Department of Chemistry, Indrashil University, Mehsana, Gujarat. India E-mail: nidhi.gour@indrashiluniversity.edu.in; gournidhi@gmail.com

[b] Department of Medicinal Chemistry, Indian Institute of Advanced Research, Gandhinagar, Gujarat, 382426, India;

[c]Department of Physics, IITRAM, Ahmedabad; E-mail: dheerajsingh@iitram.ac.in

[d] Bioengineering Discipline, Indian Institute of Technology Gandhinagar (IIT Gandhinagar),E-mail: dhiraj.bhatia@iitgn.ac.in

[e] Department of Science, School of Technology, Pandit Deendayal Petroleum University, Gandhinagar, Gujarat, India

Abstract: We report the dual-sensing properties of acyl-thiourea derivative, N-((6-methoxy-pyridine-2-yl)carbamothioyl)benzamide(**NG1**) for Cu^{2+}ion and lactic acid. The novel sensor can act both as a colorimetric and fluorescence probe for sensing Cu^{2+}ion by producing a yellow color and enhanced blue fluorescence in the presence of Cu^{2+}ion. The sequential addition of lactic acid on the other hand caused suppression of yellow color produced and also simultaneous quenching of blue fluorescence. The application of **NG1** as a selective sensor for Cu^{2+}ion and lactic acid has been assessed in detail by UV visible and fluorescence spectroscopy. Further, structural modification of the probe **NG1** suggests the crucial role of both pyridine and acyl-thiourea side chain in the binding of Cu^{2+}ion and also an important part of the O-methoxy group

in making **NG1** the most sensitive probe of its structural analogs. The experimental results of the interaction of **NG1** with Cu^{2+} ion and lactate were also validated theoretically by quantum chemical calculations based on density functional theory (DFT). The ground state geometries of the studied probes and their complexes were calculated in the gas phase at B3LYP/6-311++G(d,p) level of theory and used for the further study of molecular properties. TD-DFT calculations were performed to analyze observed UV-Vis absorption results and the calculated results were in support of the experimental findings. Finally, the ability of **NG1**for the sequential detection of Cu^{2+} ion and lactate in cellshas been studied, which suggests **NG1** can be used effectively for the cellular imaging applications and selective sensing of Cu^{2+} ion and lactate ion simultaneously. To, the best of our knowledge, this is the first report wherein a dual sensor for Cu^{2+} ion and lactate ion is synthesized and it may in all possibilities pave the way for the diagnosis of Cu^{2+}ion associated disorders like Wilson's disease and in the detection of elevated lactate levels which are associated with the wide range of pathologies like mitochondrial diseases, cerebral ischemia, and cancer.

Keywords: Copper and Lactic acid detection; colorimetric response,; Cell imaging; DFT calculations, Fluorescent sensor

Introduction

Cu^{2+} is an essential micronutrient that is utilized as a cofactor in various enzymatic process and is involved in proper functioning of plethora of biological activities.[1] However, if the concentration of Cu^{2+} increases it causes deleterious effects on kidney, liver and gastrointestinal tracts and lead to diseases like Alzheimer's, Parkinson's and Wilson's disease.[2-4] Due to the associated toxicity of increased Cu^{2+} concentration, the government agencies throughout world have set maximum permissible levels of Cu^{2+} in drinking water. U.S. Environment Protection Agency (EPA) and World Health Organization (WHO) regulate maximum permissible levels of copper (II) of less than 20 μM and 31 μM in water, respectively.[5] Hence, to test the permissible concentrations of Cu^{2+}, it is imperative to develop novel sensors which could detect Cu^{2+} in a highly selective and sensitive manner. There is growing interest to develop novel analytical techniques for Cu^{2+} detection and currently the instrumental techniques which are widely used for the detection of Cu^{2+} are inductively coupled plasma mass spectrometry (ICP-MS)[6], atomic absorption spectrometry (AAS)[7], inductively coupled plasma atomic emission spectrometry (ICP-OES).[8] These instrumental techniques are very costly and complicated to use and require sophisticated training. Hence, optical probes that could detect Cu^{2+} with colorimeter and fluorescence are in great demand since they offer simple, cost-effective methods for rapid and efficient detection of Cu^{2+} concentrations. Fluorescent chemosensor, for example, oligo-thiophene-phenylamine based Schiff's bases,[9] ferrocenes based chemosensor,[10] N-benzoyl thioureas,[11] benzimidazole subsidiaries,[12] pyridine acyl thiourea subordinates[13,] etc have been accounted for the detection of $Cu^{2+.}$

Herein, we report novel acyl thiourea derivative N-((6-methoxypyridin-2-yl)carbamothioyl)benzamide (**1**) which could efficiently detect Cu^{2+} at very low concentration both by colorimetric and fluorescence methodology. Interestingly, the color and fluorescence are quenched in the presence of lactate. Hence, probe NG**1** can also be used for sequential detection of Cu^{2+} and lactate. Lactic acid is also very harmful at concentrations above the threshold, and many diseases like mitochondrial diseases, cerebral ischemia, and cancer are associated with high lactate levels in the blood.[14] Combined experimental tools (UV-visible, fluorescence, FTIR) and quantum chemical calculations based on density functional theory (DFT) were used for the sequential identification of Cu^{2+}ions and lactic acid by probe **NG1**.[15] Finally, the

biocompatibility and application of NG1 for cellular detection of Cu^{2+} and lactate were perceived via MTT assay and cell imaging experiments. Notably, it was found that fluorescence of cells was remarkably enhanced in the presence of Cu^{2+} while it was quenched when exogenous lactic acid was added to cell culture. Hence the utility of NG1 in sequential detection of Cu^{2+} and lactate can also be surmised. (Figure 1)

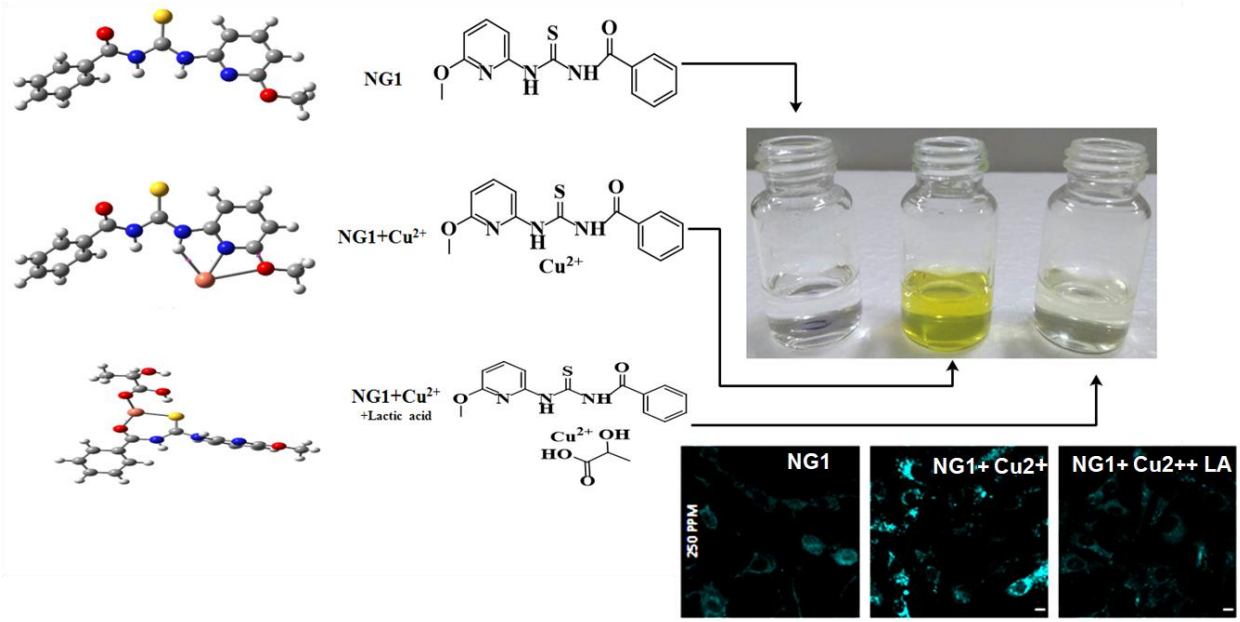

Figure 1: A diagrammatic representation of the utility of NG1 for sequential detection of Cu^{2+} and Lactate. (A) DFT computed optimized geometries of (A) (Top) **NG1**, (Middle) **NG1**+$Cu^{2,}$ and (Bottom) **NG1**+Cu^{2+}+Lactic acid;

2. Results and discussion

The chemical synthesis of **NG1** was carried out in one step by condensation reaction between benzyl isothiocyanate and 2-amino-6-methoxy pyridine via Scheme-1. The chemical structure of **NG1** was characterized by NMR, mass spectroscopy, LCMS, and its purity were ascertained by HPLC.

Scheme 1

There are reports in literature wherein acyl thiourea derivatives have been used as a probe for detection of Cu^{2+} ion[16-18] Hence, we were motivated to assess the application of **NG1** as a sensor for metal ions. Thus, to assess the sensing properties of probe **NG1**, experiments were performed

by co-incubating **NG1** with a series of divalent metal ions. Metal-ions binding study of **NG1** was carried out following the method described in the experimental section using the metal ions such as Cu^{+}, Na^{+}, K^{+}, Cs^{+}, Ca^{2+}, Mg^{2+}, Ba^{2+}, Cr^{3+}, Mn^{2+}, Co^{2+}, Ni^{2+}, Cd^{2+}, Zn^{2+}, Ag^{+}, Hg^{2+}, Pb^{2+}, Sr^{2+}, Fe^{2+}, Fe^{3+} and Cu^{2+} ions. As can be accessed from Figure 2 there was selective detection of only Cu2+ ion by NG1 and the color of the solution in a vial containing NG1+ Cu^{2+} changed from colorless to yellow.

Figure 2

Further, an interference assay was performed by mixing all metal ions except Cu^{2+} with NG1. Notably, there was no visible change in the color of the solution even in the presence of all metal ions. However, when Cu^{2+} was added to this mixture, the colorless solution changed to yellow. As revealed by the colorimetric response **NG1** produced yellow color only in the presence of Cu^{2+} and was least affected by the presence of other types of common ions (250 ppm: Na^{+}, Cu^{+}, Fe^{3+}, Cd^{2+}, Mn^{2+}, Ag^{+}, Hg^{2+}, K^{+}, Mg^{2+}, $Ca^{2+,}$ and Cr^{3+} ions). Hence it can be inferred that NG1 shows optimal activity with negligible interference by other ions (Fig S). The same results were also evaluated with UV−visible spectroscopy studies. The UV visible spectra of 50 ppm solution of NG1 reveal a broad peak with maxima from 290-320 nm. When 50 ppm Cu^{2+} was added to this solution alone sh a peak shift from 310 nm to 339.5 nm could be assessed, There was also slight enhancement of broad peak in the range of 400- 450 nm which corresponded well with the yellow color produced in the solution due to interaction between **NG1** and Cu^{2+} ions, **NG1** selectively interacts with Cu^{2+} ions and the new peak appeared in the visible region (400-450 nm) may be assigned to intramolecular charge transfer (ICT) transition (Fig. 1A and 2A).

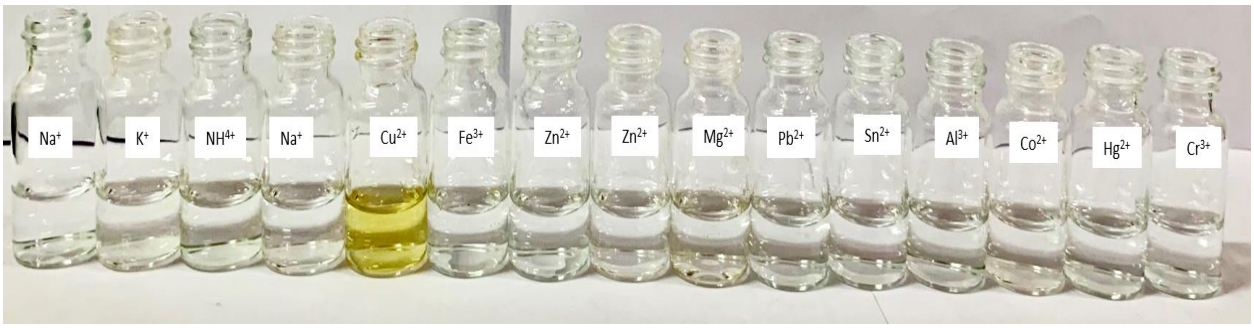

Figure 2. Vial images of **NG1** with Cu^{2+} ions and other metals showing yellow fluorescence and selectivity for Cu^{2+} ions.

To study the interaction of **NG1**with Cu^{2+}ions in more detail, the absorption spectra of the **NG1** probe was studied in the presence of different ppm levels of Cu^{2+} ions by UV−visible spectroscopy. As shown in Fig. 2A **NG1** exhibited a maximum absorption at ~310 nm. On the gradual addition of Cu^{2+} ions, the absorption intensity at ~319 nm decreases whereas an additional absorption appears simultaneously at ~340 nm through an isosbestic point at 320 nm. . The intensity of this peak at ~340 nm is increased as the concentration of Cu^{2+}ions (0-50 ppm) was gradually increased and was ascertained to the formation of aggregated complex state **NG1**-Cu^{2+} complex (Fig. 3B). The interaction is replicated in the visual color change from colorless to yellow.

To investigate the measurable response of the synthesized probe **NG1** towards Cu^{2+} ions, different concentrations of **NG1**: Cu^{2+}complex were studied. The plot shows the linear relationship in the concentration range between 2.5 to 50 ppm. The limit of detection (LOD) is detected by UV−visible spectroscopy and is calculated by the following formula.

$$LOD = \frac{3\sigma}{Slope\ of\ calibration\ curve}$$

where the σ is the standard deviation.

LOD was calculated to be 1.5 ppm from the plot of absorbance vs Cu^{2+} ions concentration.

In conclusion, the convenient visual detection limit with the naked eye for the newly synthesized probe **NG1** is 1.5 ppm for Cu^{2+}ions, which is much lower according to the maximal permitted level of Cu^{2+} ions. The short response time and high selectivity for the probe **NG1** in visual inspection could be accounted for a strong affinity towards specific Cu^{2+} ions. (Figure 3C)

The Job's plots were constructed to demonstrate complexation between Cu^{2+}ionsand probe **NG1**. The indicative of **1:1**complexation between Cu^{2+}ions and probe **NG1**. Job's plots revealed that 1:1 binding stoichiometry between probe **NG1**and Cu^{2+}ionsand suggests for bis-coordination of Cu^{2+}ionsvia nitrogen and Sulphur atom on the probe **NG1** ((Figure 3D)). Moreover, the interaction and binding behavior between probe **NG1** and Cu^{2+}ionswas also evinced via FTIR and was presented in supporting information (Fig. S2). FTIR spectrum supported the change in characteristic peaks of probe **NG1** in aromatic region (1450-1650 cm^{-1}) due to interaction via nitrogen and sulfur atoms on the probe **NG1** with Cu^{2+} ions which proved the **NG1**-Cu^{2+}complex formation. Thus, the present study realizes that the probe **NG1** can be used for the simultaneous detection of Cu^{2+} ions in real water samples as well as it could be potentially used for sensing Cu^{2+} ions in mammalian cells and organisms.

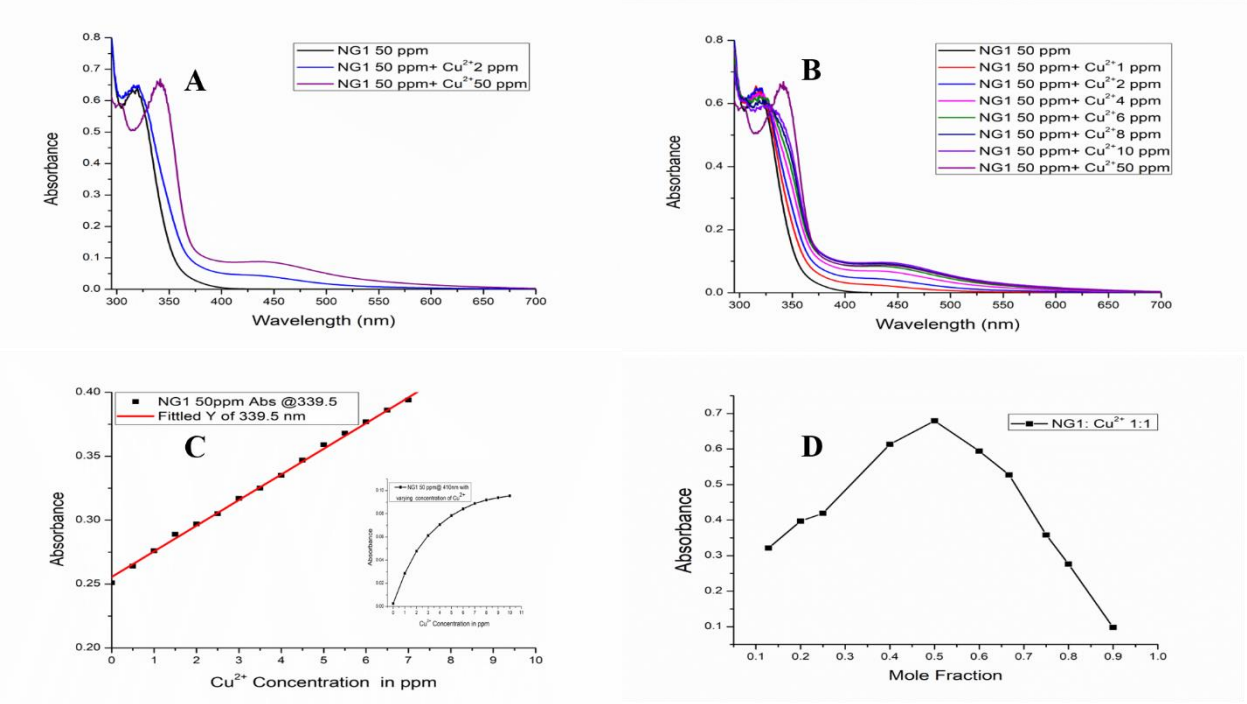

Figure 3.A)UV-visible spectra of probe**NG1** with and without Cu^{2+} at 50 ppm concentration; **B**) UV-visible spectra of probe **NG1** after sequential addition of Cu^{2+}; **C**) LOD of detection of probe **NG1** by colorimetry;**D**) Job's plot was drawn a taking a fixed concentration of probe **NG1** and varying concentrations of Cu^{2+} ions show 1:1 stoichiometry.

Once the sensitivity and selectivity of probe **NG1** were ascertained by colorimetry, fluorescence assay was performed in the presence of Cu^{2+} ions. Interestingly, it could be determined that **NG1** also exhibited excellent fluorescence emission properties. When **NG1** was excited at 353 nm the emission spectra were obtained with the maxima at 440 nm. When Cu^{2+}ionswas added in increasing concentration there was a significant enhancement in the fluorescence intensity and the graph exhibited a redshift towards 470 nm. (Figure 4)

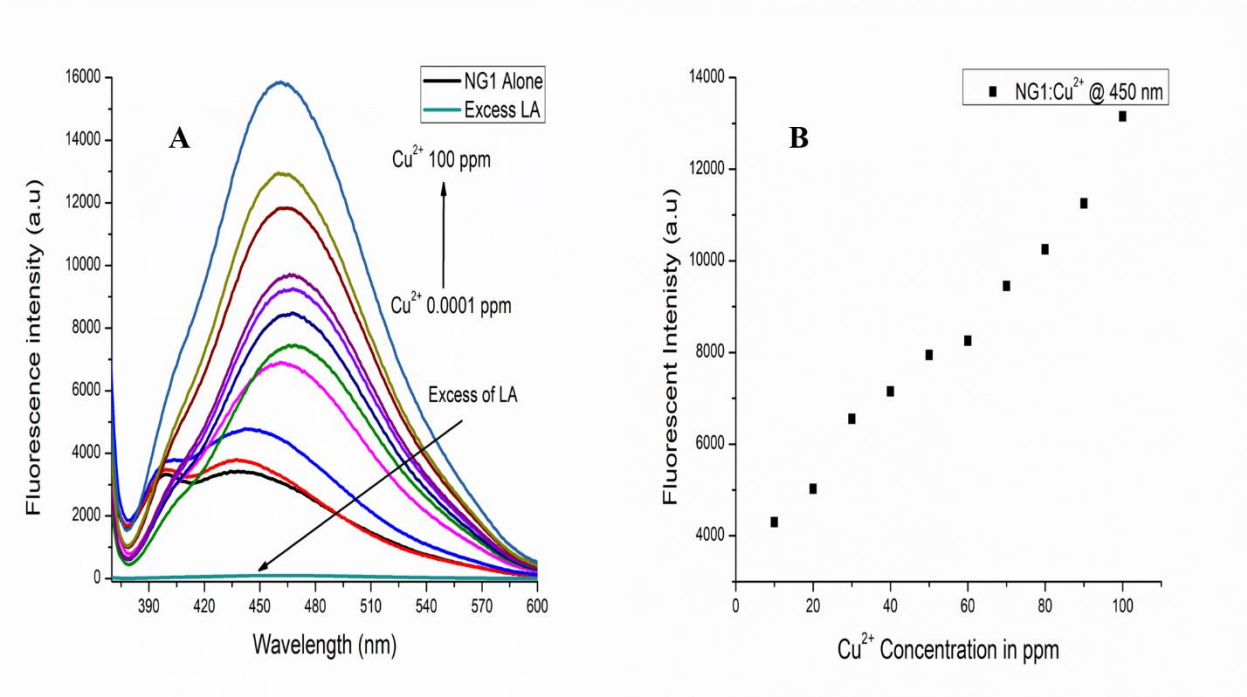

Cu^{2+} concentration	Copper citrate	Couper lactate
0.001	3402.788	3402.788
0.01	3433.675	3403.225
0.1	3775.450	3418.363
1	4727.056	3437.394
10	5935.344	3441.824
100	13764.67	3445.794
1000	21281.342	3459.444

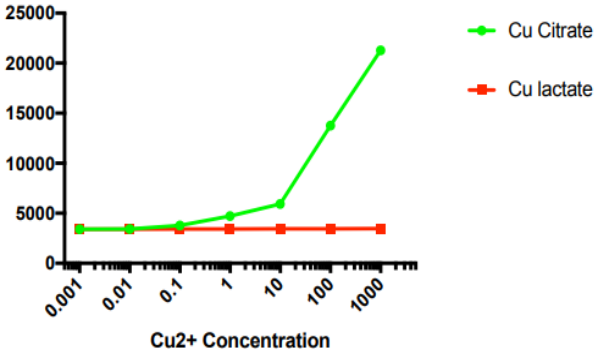

Figure 4. A) Fluorescence spectra of **NG1**(1mM) against a varying concentration of copper lactate from 0.001-100 ppm;**B**) The curve plotted with the fluorescence intensity of **NG1** at *440* nm versus Cu^{2+} ions concentrations (10 ppm–100 ppm) from C showed a steady increase in fluorescence as the concentration of Cu^{2+} ions increases;**C)** Table of fluorescence intensities enhancement on the addition of increasing concentrations of Cu^{2+}ions using two different salts copper citrate and copper lactate; ;**D)**Fluorescence graph shows no enhancement on the addition of copper lactate in increasing amount on the other copper citrate showed a steady increase in fluorescence.

In our body, copper mainly exists in the form of copper citrate. However, copper also plays an important role in regulating blood lactate levels and forms copper lactate complex inside the body. Hence. we decided to perform titration studies on the interaction of NG1 with copper nitrate and copper lactate Interestingly while Cu (II) citrate showed a steady increase in fluorescence the Cu (II) lactate salt was not able to bind **NG1** and no increase in fluorescence was observed. This study indicated that Cu(II) lactate complex was more stable and hence Cu^{2+} ions could not form complex with**NG1** and induce a color change. (Figure 4)

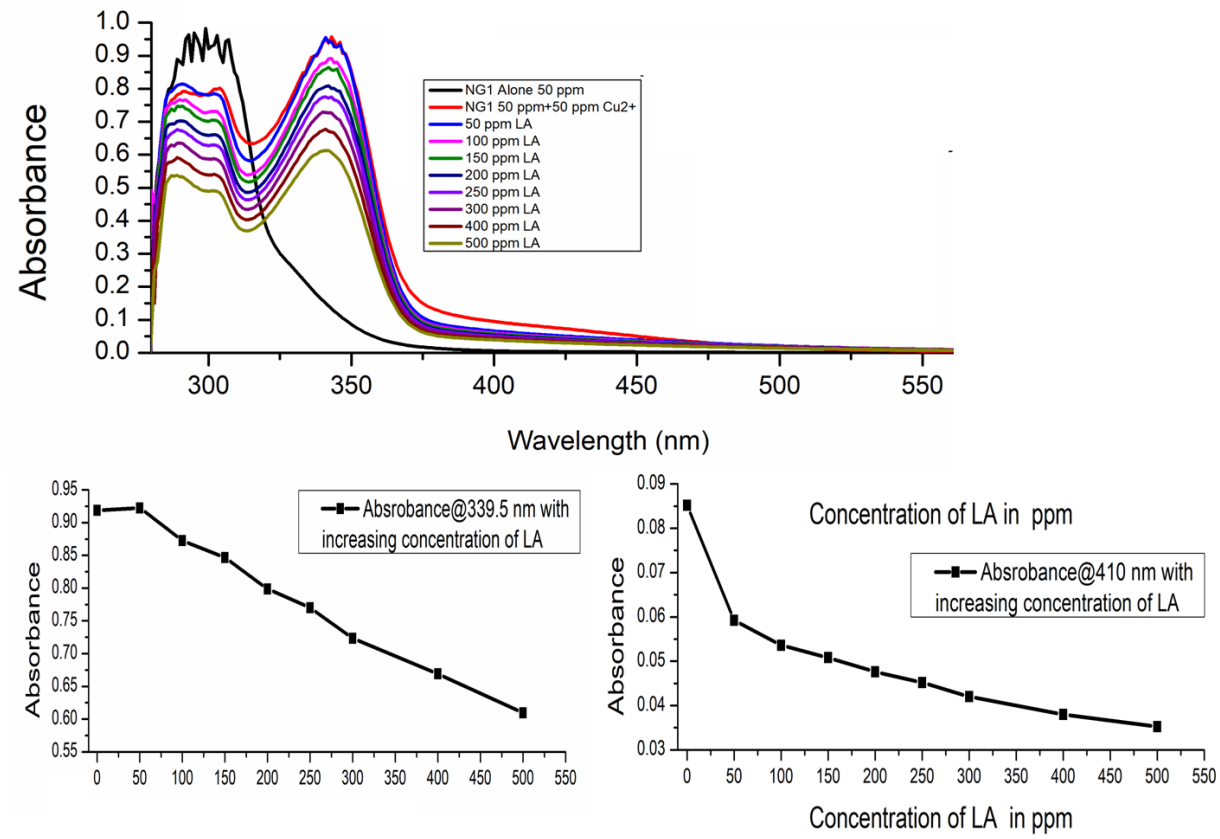

Figure 5. **A**) UV spectra of **NG1**in the presence ofCu^{2+}ions and varying concentration of lactic acid (0ppm -500 ppm); **B**) UV spectra of **NG1: Cu^{2+}**complex against the varying concentration

of lactic acid from 0 to 500 ppm at Wavelength 339.5 nm **C**) UV spectra of **NG1: Cu^{2+}**complex against the varying concentration of lactic acid from 0 to 500 ppm at wavelength 400 nm

Hence, motivated by these results we decided to assess the application of **NG1** for sequential detection of both Cu^{2+}ions and lactic ions. For sensing of lactate ions, solutions of **NG1-**Cu^{2+}Complex (50ppm) was prepared in 70 % Methanol in water. Then solutions of lactic acid were prepared (5000 ppm stock solution) in Milli -Qx water. Then 0 to 500 ppm Lactic Acid was mixed with of complex solution in a 3 mL in the vial and the reaction mixtures were incubated for 10 minutes. The UV -Vis spectra of all these solutions were recorded after incubation and those were compared to the spectrum of Cu^{2+} complex of the same concentration but without any Lactic acid to ascertain the selectivity. The experiment revealed that the **NG1-**Cu^{2+} Complex is selectively interacting with Lactic Acid. Then UV -Vis titration with lactic acid was carried out following a similar procedure as described above for UV -Vis titration of **NG1** with Cu^{2+} ions, except instead of Cu^{2+} ions, Lactic Acid was added into the solution of the Cu^{2+} complex. (Figure 5)

Figure 4B and 4C how that decrease in absorbance on increasing concentration of lactic acid in the 50 ppm **NG1**: Cu^{2+} yellow complex from 0 to 500 ppm, which shows the color changes of yellow complex become colorless at higher concentration of lactic acid.

Further to understand the role of acyl thiourea conjugate in sensing two other analogs structural probes of **NG1**, **NG2** and **NG3** were synthesized (Scheme 1, bring old scheme which you draw). Interestingly, both probe **NG1** and **NG2** show selective sensing for Cu^{2+}ions, However, probe **NG3** showed very little sensitivity for Cu^{2+} ions. The order of sensitivity of **NG1** for the

detection of Cu^{2+} ions was in order**NG1**>**NG2**>**NG3**. The observation suggested a crucial role of pyridine in binding Cu^{2+} ions due to NG1 and NG2 has more sensitivity than NG3. Further, since **NG3** could also sense Cu^{2+} ions, it may be inferred that thiourea moiety can also participate in complex formation with Cu^{2+}ions. Since **NG1** revealed higher sensitivity as compared to **NG2,** a crucial role of –O methoxy group for increasing sensitivity could also be deciphered. The methoxy group is know to have electron releasing properties. The lone pairs of methoxy groups present in NG1 may be involved in the resonance and could attribute to an increase in the electron density around the Sulphur and oxygen atom. Hence, Sulphur and oxygen atoms in NG1 can easily donate its lone pairs of electrons to Cu^{2+} and cause its effective binding leading to the yellow color complex formation.

Further, to perceive a greater insight into the complex formation by **NG1** and its structural analog **NG2 and NG3** with $Cu^{2+}$and lactic acid we resorted to validate theoretically the experimental results by quantum chemical calculations based on density functional theory (DFT). We have conducted a comparison study on these three probes (**NG1**, **NG2,** and **NG3**) and their complexes with the Cu^{2+} ion and Lactic acid. DFT calculations are performed at B3LYP/6-311++G(d,p) level of theory for these probes and their complexes in the gaseous phase. The vibrational frequencies were also calculated for all the studied structures, where the optimization converged successfully to the shallow local minima on the potential energy surface, which was confirmed by the absence of negative/imaginary vibrational frequencies.Fig.10shows that the ground state optimized geometry of all three probes and their association with Cu^{2+} as well as lactic acid. The binding energy (BE) of these complexes are elucidated as:

$$BE = E_{complex} - \Sigma E_{individual} (1)$$

Where $E_{complex}$contains represents the ground state energy of complex and $\Sigma E_{individual}$contains indicates the sum of the ground state energies of all the molecules in a particular complex. The BE of all the optimized structures is presented in curly braces in Table 1.

Table 1. Optimized energy (in Hartree) and binding energy (in kcal/mol) of the Complex **NG1** (**NG2** and **NG3** in ESI)

	Optimized Energy (Hartree)	Position 1 with Cu^{2+} (Hartree)	Position2with Cu^{2+} (Hartree)	With Lactic Acid (Hartree)
NG1	-1254.4797	-2894.9918 {-25.07}	-2894.9658 {-8.71}	-3238.7456 {-87.05}

The binding energies in kcal/mol are provided in curly braces.

Initially, the pristine robes i.e. **NG1**, **NG2**, and **NG3** were optimized using DFT calculations. Based on energetic stability, **NG1** was found to the most stable ligand. To make a better comparison, along with **NG1** other two probes (**NG2** and **NG3**) were also interacted with Cu^{2+} and lactic acid (see Fig. 10). There were at least two different possibilities interaction of Cu^{2+} with probes, one with the sulfur atom (represented as probe+Cu(1))and another one is near the nitrogen atom (denoted as probe +Cu (2)) as can be seen in Fig. 10. After the interaction and geometry relaxation process, it is noteworthy that in all the six complexes (probes + Cu(1), Cu (2)), Cu^{2+}tend to strongly bind with Sulphur atom of all the studied probes (**NG1**, **NG2,** and **NG3** with Cu (1)) as shown in Fig. 10. This trend is also confirmed from the binding energies which are higher for all the probes + Cu (1)complexes than probes + Cu (2). The BE calculations for all complexes(with Cu) indicate that the complex **NG1**+ Cu(1)is the most stable complex.

Nevertheless, the BE of **NG1**+ Cu(1) is -25.07 kcal/mol which is slightly higher in comparison to **NG2**+Cu(1) complex. This small energy difference is considerable here because in experimental observationall the three probes give yellow color after incorporating the Cu but the only key difference is between these three probes were their concentration. For probe **NG1**, presence of only 1.5 ppm concentration of Cu^{2+}causes the occurrence of yellow colour but in case of other probes (**NG2** and **NG3**) yellow colour appears only after the incorporation of high Cu concentration. So,for further studies we have selected **NG1**+Cu (1) complex on the basis of BE to validate our experimental findings.

Here, the Cu^{2+}strongly interacts with the oxygen and sulfur atoms having a bond length of 1.95Å and 2.18 Å (see Fig. 10). In complexes 2 (all the three probes), Cu^{2+} is weakly coordinated with nitrogen and oxygen atoms as bond length increased on the interaction (see Fig. 10). We have also optimized a dimer like structure of **NG1** with single Cu^{2+} atom (Fig.11(c))to check the assembly of Cu^{2+} with more **NG1** molecules and almost similar structural features are found as in the single case where Cu^{2+}interacting with S atom of another **NG1**.

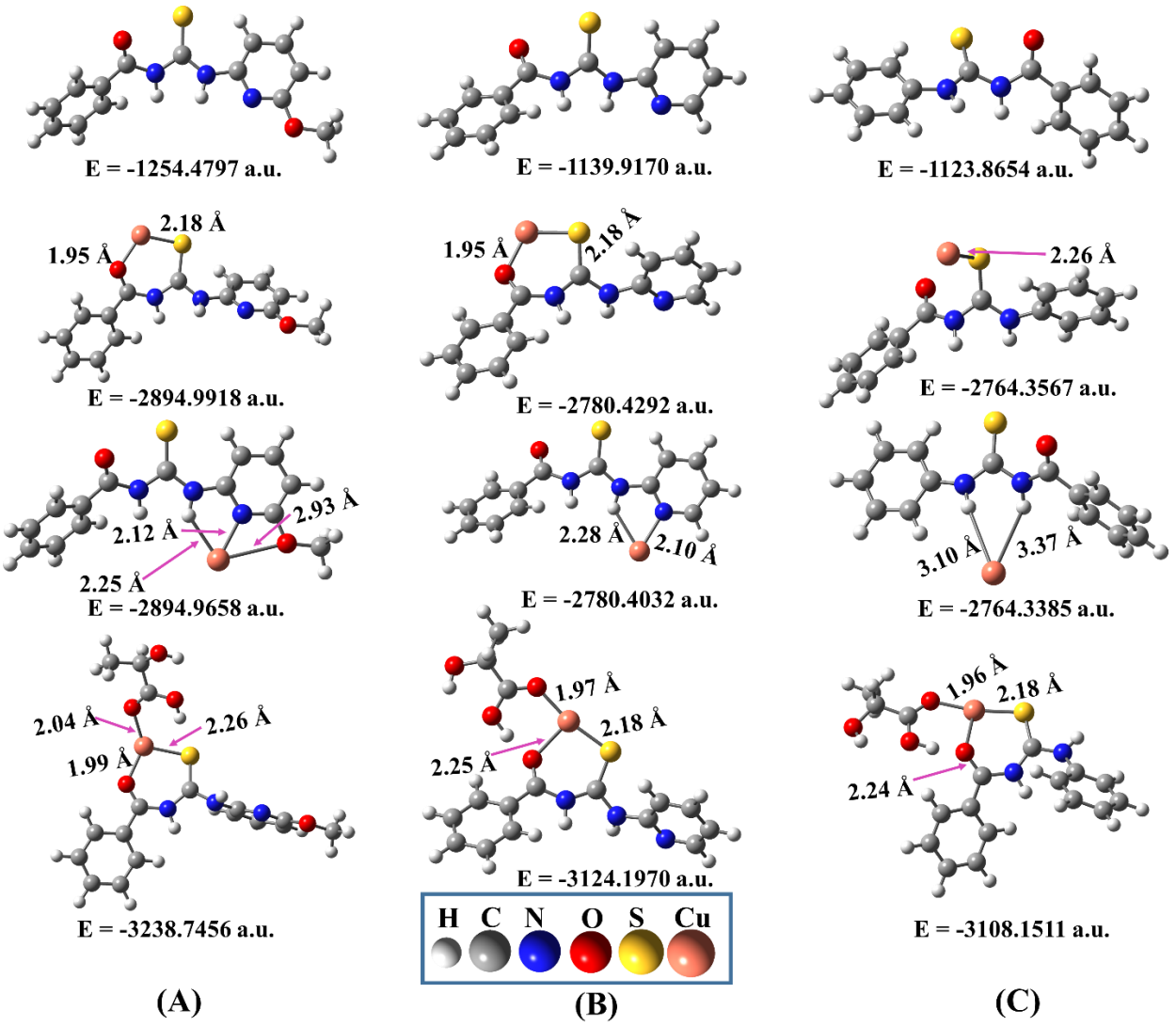

Figure 6:DFT computed optimized geometries of (A) **NG1**, **NG1**+Cu(1), **NG1**+Cu(2) and **NG1**+Cu^{2+}+Lactic acid, (B) **NG2**, **NG2**+Cu(1), **NG2**+Cu(2) and **NG2**+Cu^{2+}+Lactic acid, and (C) **NG3**,**NG3**+Cu(1), **NG3**+Cu(2) and **NG3**+Cu^{2+}+Lactic acid with their optimized energy in Hartree.

As experimentally observed, as a result of the interaction of Cu^{2+} with **NG1**a yellow colored complex is obtained but when lactic acid is incorporated with this complex this yellow color quenches. To understand this behavior, we have introduced a molecule of lactic acid with this stable complex of **NG1**+Cu (1) and it can be seen in Fig.10(a). From Fig.10a (compare the structure of second and fourth geometry from the vertical position) it is noticeable that Cu^{2+} is

strongly binding with the sulfur and oxygen atom of **NG1** through 2.18 Å and 1.95 Å respectively. However, upon complex formation with lactic acid both the bond strengths get weekend and calculated to be 2.26 Å and 1.99 Å respectively. Also, it can be noticed from Fig. 11 (a) that Cu form a strong bond (2.20Å) with the oxygen atom of -C=O of carboxylic group in a lactic acid molecule. But after complex formation of **NG1**+Cu (1)with lactic acid, this bond gets stronger with new bond length of 2.04Å as can be seen in Fig. 11 (b). Another noticeable feature is the least BE of this complex (**NG1**+Cu^{2+}+Lactic acid) in comparison to the other complexes. The BE of this complex is -87.05 kcal/mol which is much lower than the -95.86 kcal/moland -112.49 kcal/mol for **NG2**+Cu^{2+}+Lactic acid and **NG3**+Cu^{2+}+Lactic acid, respectively.It is a clear indication of Cu^{2+} binding with lactic acid and alters the property of **NG1**+Cu (1)complex due to the formation of copper lactate and decolorized.Also, it promotes the regeneration of self-assembly of **NG1**.Furthermore, electrostatic potential mapped surfaces were generated to elucidate this behavior in terms of charge densities.

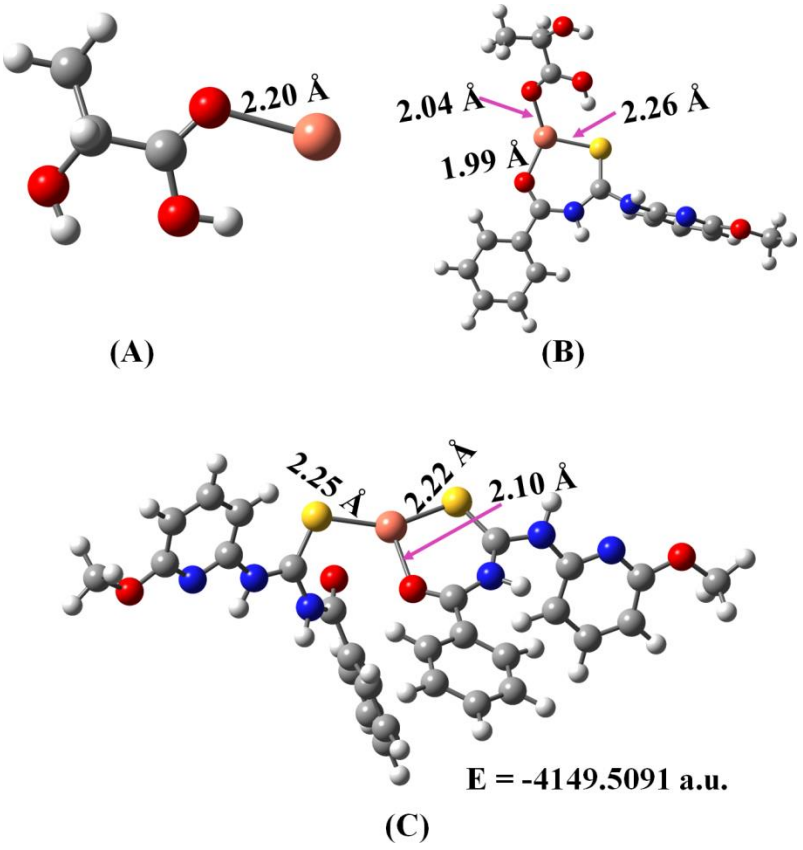

Figure 7. Optimized structures of (A) Lactic acid with Cu^{2+}, (B) Probe **NG1** with Cu^{2+} and Lactic acid, and (C) self-associated dimer of **NG1** bonded to single Cu-atom.

3.4.2 Electrostatic Potential (ESP) Mapped Electron Density Surfaces

Molecular electrostatic potential (MEP) (also called ESP) of a molecular association is correlated with the corresponding partial charges, dipole moment and chemical reactive sites. The mapping of any molecular system is the way to visualize the relative polarity of the studied molecules. The expression for the ESP at any point *r* in the space near the molecule is given by

$$V\ (r) = \sum \frac{z_A}{|R_A - r|} - \int \frac{\rho(r\prime)dr\prime}{|r' - r|} \quad (2)$$

where, Z_A is the charge on the nucleus *A* studied at R_A and $\rho(r')$ the electron density. For probe **NG1** and complex **NG1**with Cu and lactic acid, the electron density iso-surface on which the

ESP surface was calculated and mapped is shown in Fig. 11. Recently, ESP mapping has played a remarkable role in geometrical arrangement, charge density analysis and polarity of different molecular systems [25-28]. Generally, MESP reflects the relative polarity of the molecule as positive potential indicates the electrophilic sites while adverse potential indicates the nucleophilic attack sites.To visualize the electrophilic and nucleophilic sites in these complexes, the MESP was generated on DFT minimized structures at B3LYP/6-311++G(d,p) level of theory.

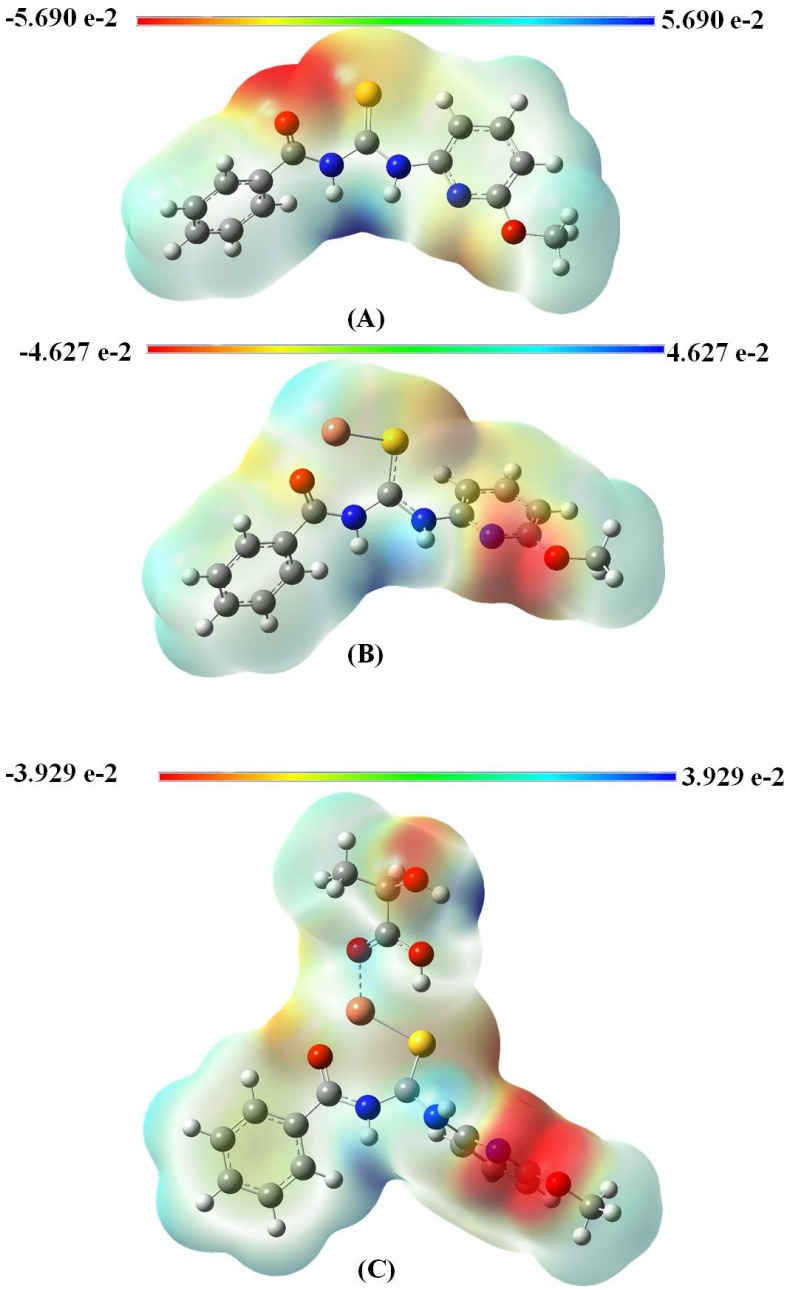

Figure 8. Electrostatic potential surfaces plotted from the total self-consistent field (SCF) density having iso-value MO = 0.020000, density = 0.000400, calculated at the B3LYP level of theory. (a) **NG1**, (b) **NG1** with Cu^{2+} and (c) **NG1** with Cu^{2+} and Lactic acid.The red color indicates the most electronegativity, the blue color shows the most positive election density and the area of zero potential on the molecular surface represented by green color.

As shown in the top panel of mapped optimized structure, the potential increases in the color code. The charge distribution over the pristine**NG1** with Cu^{2+} and lactic acid is visualized in the ESP map in Figure 12. Also, the MESPs of **NG2** and **NG3** are in ESI. In pristine**NG1**, nitrogen, oxygen, and Sulphur are the three electronegative atoms, so it can be noticed a negative charge distribution over both the oxygen as indicated by the red color whereas blue color over the benzene ring and both the nitrogen atom near Sulphur group indicates low electron density (Figure 10(a))as these atoms are less electronegative than oxygen. Shape and charge distribution are found to be considerably different in **NG1** with Cu^{2+} atom and lactic acid. Positive charge increases (blue color near the Cu atom) as Cu^{2+} atom attaches with Sulphur in comparison with the pristine**NG1** and negative charge increases near the oxygen atom which is attached with $–OCH_3$ group. Ongoing from **NG1**-Cu^{2+} complex to **NG1**-Cu^{2+}-lactic acid, the positive charge increases around the Cu^{2+} atom as Cu^{2+} is binding with the oxygen atom of the carboxylic group of lactic acid. The reason may be due to charge transfer from Cu^{2+} to oxygen atom as it is known that Cu^{2+}form copper lactate with lactic acid. This result clearly indicates that Cu^{2+} is interacting more with lactic acid than the probe as yellow color of **NG1**-Cu^{2+} quenches after interacting lactic acid which is experimentally observed.

3.4.3 Electronic absorption

Time dependentdensityfunctional theory (TD-DFT) calculated results were used to explain the experimentally measured absorption bands of the complexes**NG1**and **NG1**with Cu^{2+} in the presence of different ppm of Cu^{2+}.TD-DFT calculations of**NG1**and **NG1**with $Cu^{2+}$was performed using DFT calculations in the gas-phase. The frontier molecular orbitals of pristine**NG1** and with Cu^{2+}, are shown in Fig. 13.Quantum chemical calculations show that the **NG1** reveals three bands at 427, 325, and 311 nm (experimentally observed at 290 nm in 70 % Methanolin water).

The theoretically calculated absorption at ~325 nm red-shifted when Cu^{2+} is added and absorption appears at ~680 nm, which shows a similar trend as of experimentally observed absorption bands. Energy bands calculated at ~325 and ~680 nm with oscillator strengths (f) 0.0844 and 0.1445 are due to electronic excitations from HOMO-1→LUMO and HOMO→LUMO+1 which are attributed to electron transfer from Sulphur atom to another part of **NG1**and from Sulphur to Cu^{2+} atom, respectively. For both complexes (pristineprobe **NG1** and **NG1** with Cu^{2+}-atom, the calculated bands are in good agreement with observed absorption bands and show a similar trend.Overall, nice correlation is observed between experimental UV-Vis absorption and TD-DFT calculated absorption data.

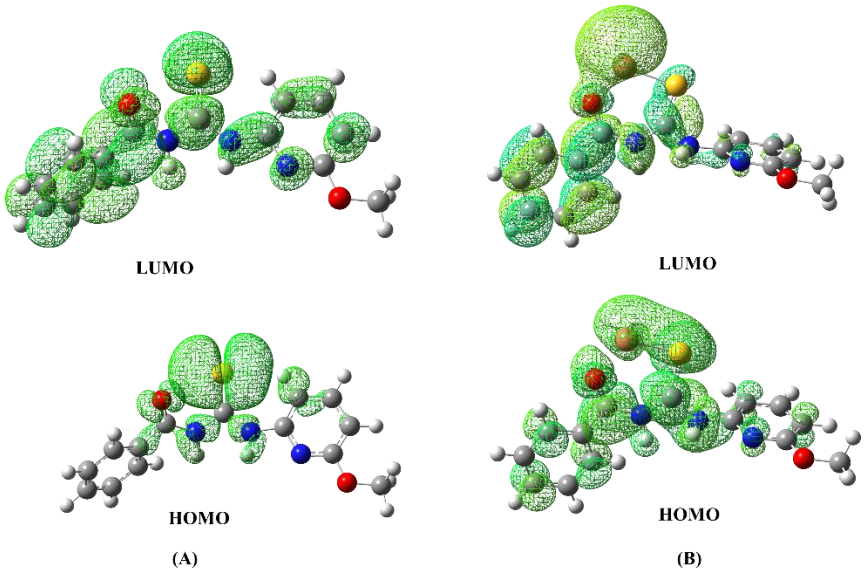

Figure 9. Molecular orbitals HOMO and LUMO of (A)pristine**NG1** and (B)**NG1** with Cu^{2+}. The orbitals were obtained using an iso-surface value of 0.02 e/$Å^3$.

.**Cellular detection of Cu2+ and lactate using NG1-Cu^{2+} complex**

The *invitro* sensing capabilities for **NG1**-Cu^{2+} were further explored by testing its capacity to sense Cu^{2+} and lactate in mammalian cells. The application of **NG1-Cu^{2+}**complex was tested in

living cells by using MTT cytotoxicity assay and cellular imaging.Upon studying the robustphotophysical properties of these novel RGB emitting compounds, we decided to test for their biocompatibility and they are *in cellular* behavior.Cell viability was measured by measuringthe absorbance of MTT at 570nm and calculated the ratio of absorbance of cells treated with respective compounds to that of control untreated cells. The results shown in **Fig.xx**indicate that**NG1** compounds have minimumcytotoxicity in cells (~80% cell viability), strongly suggesting that these compounds can be further exploitedfor cellular imaging applications. MTT assays were carried out using a stock solution of 500:500 ppm **NG1**:Cu^{2+}. The stock was serially diluted and cells were grown in well containing 25, 50, 75, 100, 150, 200, 250 **NG1**:Cu^{2+}complex in ppm.

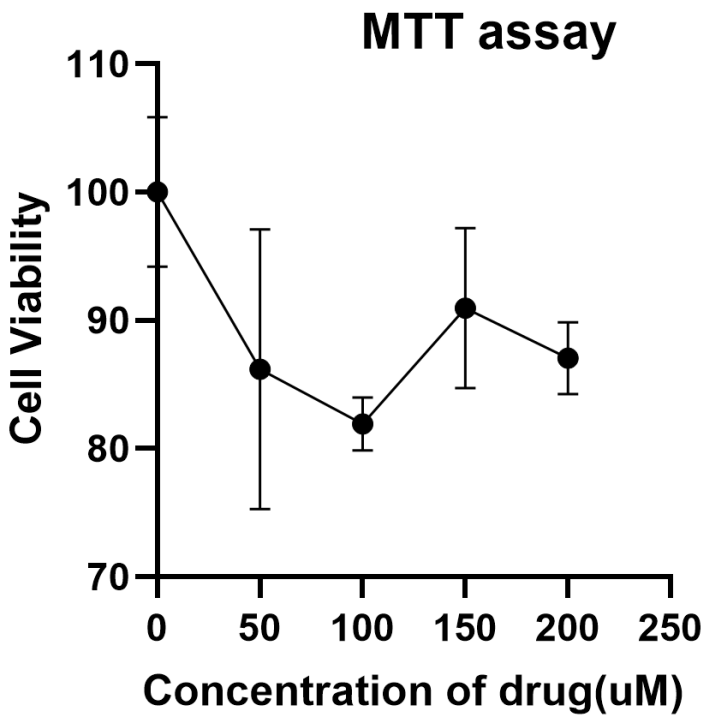

Fig. xx: Cytotoxicity measurements on RPE1 cell using NP1 molecule. Cells were treated with different concentrations of NG1 and the cell viability was calculated using MTT assay. (n = 2 experiments with 10,000 cells in each condition)

To test for cell permeability and fluorescence property of **NG1**molecule in cells, experiments were carried out using retinal pigmented epithelial (RPE1) cells. The cells were

pulsed with **NG1** in the absence or presence of different concentrations of Cu^{2+} for 15 mins, fixed and imaged on the confocal microscope. Following*in vitro* data, imaging of fixed cells using a confocal microscope displayed that these compounds are permeable in cells and show bright blue fluorescence in the blue filter (shown in **Fig.yy**).Interestingly, the fluorescence of the dye **NG1** was highly enhanced in the presence of exogenous Cu^{2+}. This enhancement in the cellular intensity of dye was rescued to background levels in the presence of lactic acid, indicating the potential of dye to sense both Cu^{2+} and lactate from cells

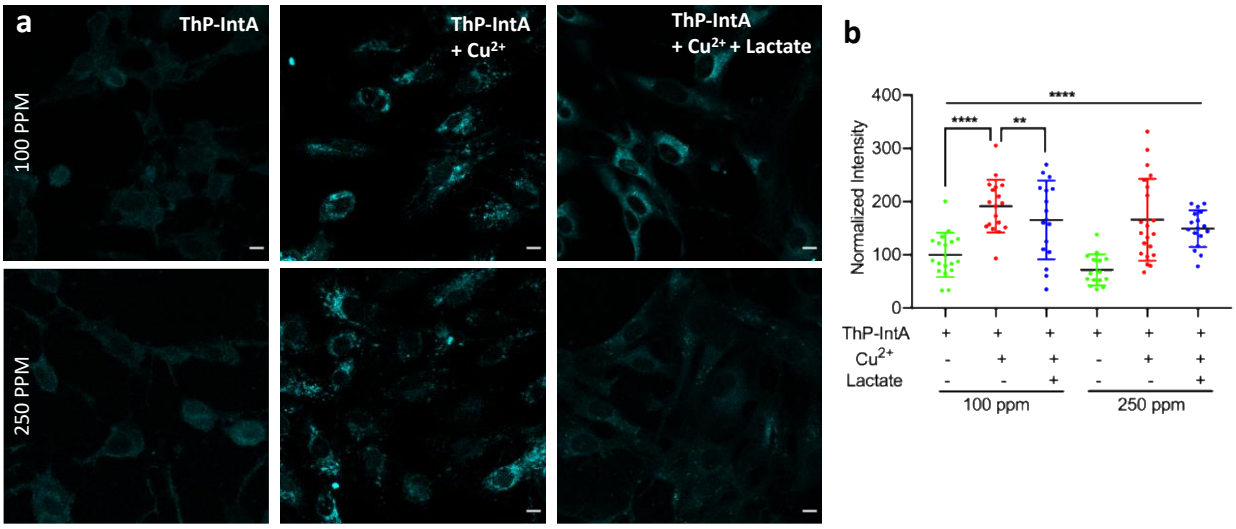

Figure 10:

Cellular imaging of Cu2+in RPE1 cells withNG1-Cu^{2+} complex. Retinal epithelial pigmental cells (RPE1) were pulsed with 100 and 250 ppm of**NG1** dye in the absence or presence of Cu^{2+} in a 1:1 ratio of dye:Cu^{2+}. Further, the cells were incubated with lactate in presence of dye and Cu^{2+} for 15 min at 37°C, fixed with paraformaldehyde, and imaged on the confocal microscope using 405 nm excitation laser and imaged acquired using broad width band-pass filters. **b.**The images were further quantified using image-J for the cellular intensity of dye in various conditions and the normalized intensity plotted inthe right fig. Scale bar: 10 μm.

Experimental section

2.1 Materials

All the starting materials for **NG1** synthesis were obtained from commercial suppliers and used as received. 2-Amino-6-methoxypyridine and Benzoyl isothiocyanate were purchased from Combi-Blocks, USA. Acetone, THF, all-metal ions were purchased from Sisco Research Laboratories (SRL), India.$Cu(NO_3)_2$.2.5 H_2O and $CuCl_2$. $2H_2O$ was purchased from Sigma. Lactic acid was purchased from Fluka.Moisture sensitive reactions were performed under an atmosphere ofnitrogen. All the solvents used for reactions were distilled before use. The water used for all the microscopy and spectroscopy measurements was ultra-pure obtained from Millipore Direct-Q® 5 UV Water Purification System. Column chromatography was carried out on silica gel (200–300 mesh). The $R_f$was recorded in Analytical TLC Silica Gel $60F_{254}$ purchased from Merck (Germany). The melting point of **NG1** and its derivatives was recorded in Visual Melting Range Apparatus (MR-VIS) provided by LAB INDIA. ^{1}H NMR (400 MHz) and ^{13}C NMR (100 MHz) spectra were recorded on an Avance III 400 NMR spectrophotometer. Proton chemical shifts were reported in parts per million concerning TMS. HPLC was done using the Waters E2695 instrument. HPLC was performed using ammonium bicarbonate buffer (ABC) with 27 minutes run time and water: ACN as mobile phase in C-18 Column. LC-MS was obtained on a Waters 2690 LC-MS instrument. The method used was Ammonium bicarbonate Buffer (ABC); 7 minutes run time and water: ACN as mobile phase in C-18 Column. UV-visible spectra were recorded on a LAB INDIA UV-Vis Spectrophotometer 3000+ with a 10 mm quartz cell at 25 ^{0}C.

2.2 Synthesis of probe NG1

In a three-necked round bottom flask, fitted with a dropping funnel 50ml of dry acetone was filled. 5.0g (27 mM) of 2-Amino 6-Methoxy pyridine was placed followed by dropwise addition of dry acetone under N_2 atmosphere during the constant stirring of the reaction mixture. Next, 7.2 g (44mM) of benzoyl isothiocyanate was added and the reaction mixture was then allowed to stir for another 2h at room temperature.The progress of the reaction was monitored by analytical TLC by using the ethyl acetate-hexane (3:7) solvent mixture. After the completion of the reaction, the reaction mixture was then poured carefully with stirring into 500 ml of cold water and the resulting yellow precipitate of (N-((6-methoxypyridin-2-yl)carbamothioyl)benzamide) is separated by suction filtration followed by washing of precipitate with water(3x100 ml). The filtrate was further purified by vacuum distillation which yielded the desired product (10.0 g, 34mmol, yields 86 %) as solid light yellow material.M.P.136 ^{0}C Rf 0.53, (This material was used in next step without any further purification) and **NG1**wasalso confirmed by EI- MS. The mass spectrum of**NG1** shows a strong molecular peak at $M^+ + 1$=287.86. While the $M^+ + 1$ ion appears for the base peak. Similarly, **NG2** and **NG3** was synthesized using aminopyridine and aniline respectively as substrate (Details of **NG2** and **NG3**syntheses is in ESI)

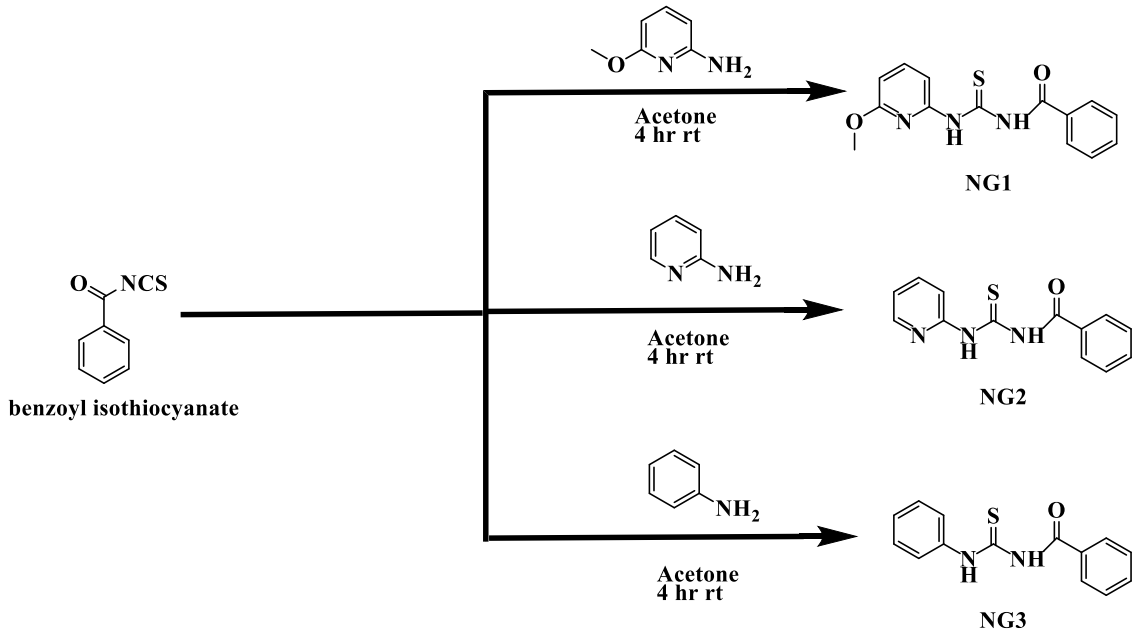

Scheme 1. |Schematic representationof thesynthesis of the probes **NG1.**

2.2 Self-assembling properties of NG1:

The self-assembly property of **NG1** assessed by optical microscopy, phase contrast, green and red filter at the 10-uMconcentration, further, to understand the mechanisms of formation of self-assembly at supramolecular state, self-assembly was characterized by Scanning electron microscopy and Atomic force microscopy, UV, FT-IR, NMR. All the study shows that the assembly is formed by hydrogen bonding, π- π stacking, electrostatic interaction, and hydrophobic interaction.

2.3 Colorimetric Detection of Cu^{2+}

For colorimetric measurements, stock solutions of 500 ppm **NG1** and 500 ppm$Cu(NO_3)_2.2.5$ H_2O. were prepared. The sensitivity of probe **NG1** for Cu^{2+} and other metal ions were tested by

mixing 250 ppm probe **NG1** with 100 ppm metals (100 ppm: Cu^{2+}, Fe^{3+}, Cd^{2+}, Mn^{2+}, Ag^{+},Hg^{2+}, Ca^{2+}, Cr^{3+}, K^{+} , Mg^{2+} and Na^{+}). The LOD of probe **NG1**was detected by making a complex of 250 ppm:250 ppm **NG1**: Cu^{2++} complex. The stoichiometric ration of **NG1**: Cu^{2+} complex was determined by adding varying concentrations of Cu^{2+} (0.5-50 ppm) to 50 ppm **NG1**.

2.4Fluorometricassay for the detection of Cu^{2+} ions and lactic acid

For fluorometric measurements, 250 ppm of **NG1** stock was used and varying concentration of Cu^{2+} (0.001-100 ppm) was added. For lactic acid-mediated quenching 250 ppm of lactic acid was added to 250ppm:100 ppm **NG1**:Cu^{2+} complex.

2.5 Computational Details

The prediction of certain important molecular properties of the ligand**NG1, NG2 and NG3** and their possible complexes with Cu^{2+} and lactic acid are calculated using density functional theory (DFT) calculations. All computational calculations were carried out using the *Gaussian 16* programming package in the presented works [15]. *GaussView 6* software was used to generate the input molecular structure and to analyze the output of all calculated results [15]. Geometric optimization calculations were performed in the gas phase using DFT by employing the internally stored 6-311++G(d,p)[23, 24] and the hybrid density functional theory that incorporates B3LYP correlational functional[25, 26]method. In general, B3LYP is a prominent method and preferable to the HF and MP2 method as it includes Becke's three-parameter exchange with Lee, Yang, and Parr's correlational functional as well as an HF exchange term. DFT calculations using the B3LYP protocol has been provided a meaningful and nice correlation with experimental results[27-30]. Time-dependent density functional theory (TD-DFT) haswasalso

incorporated to compute electronic excitation energies and molecular frontier orbitals to analyze the charge transfer from Cu to probe. Besides, the mapping surfaces for 1 with electrostatic potential (ESP) werealso shown to better understand the distribution of charges through shape, size and color code.

2.6**Cytotoxic assay:**To evaluate the biocompatibility of **NG1**, we performed a standard colorimetric MTT assay. Monkey kidney fibroblast cells were seeded at a density of 5 x 10^3 cells/well into 96-well plates and maintained in Dulbecco's modified Eagle's medium (DMEM) containing 10% fetal bovine serum (FBS) at 37^{o}C in a 5% CO_2incubator. After 24hrs once the cells have adhered to a surface, the culture medium was replaced by fresh culture medium containing varying concentrations of **NG1** compounds and again incubated for 24hrs at 37^{o}C in a 5% CO_2incubator. After incubation, the medium was aspirated and replaced by 100µl/well of MTT prepared in DMEM medium to a final concentration of 0.5 mg/mL and the plate was incubated furthermore 4 hrs at 37^{o}Cin a 5% CO_2incubator. The formed formazan crystals were solubilized by adding 100µl of cell culture grade DMSO per well and incubated for 2hrs at 37^{o}Cin a 5% CO_2incubator. The plate was gently shaken, and then the absorbance of purple formazan was recordedat 570 nm using a plate reader.

2.7 **Cellular sensing of Cu^{2+} ions:** Retinal pigmental epithelial cells (RPE1) were Cells were seeded at a density of 1.5 x 10^5 cells/well in Dulbecco's modified Eagle's medium (DMEM) containing 10% fetal bovine serum (FBS) and incubated at 37^{o}C in a 5% CO_2 incubator for 24 h. The medium was replaced with 20mM HEPES buffer and incubated with **NG1**±Cu^{2+}± Lactic acid in the concentrations of 100 ppm and 250 ppm for 15 mins at 370C in water. Post incubation, the cells were washed with ice-cold PBS++ to block endocytosis and removed the unbound dye and Cu^{2+}ions. The cells were then fixed using 4% Paraformaldehyde for 10 mins at

room temperature. The fixed coverslips were visualized for dye uptake using Leica SP8 confocal microscope. The cells were excited using 405 nm with very low laser power (~ 1% laser power) and the images were acquired using a broad width emission spectrum to capture the maximum of the emitted photons.50-60 cells were imaged in every condition using the same laser power and imaging conditions.

Data analysis: Image analysis and quantification were performed using Image-J software (nih.gov). 50 cells were randomly selected to perform the quantification. The value of the total fluorescence intensity of each cell wasobtained from Image-J. The images were quantified by subtracting thebackground and measuring the cellular intensities by measuring the areas of the cells and the total cellular intensity. The normalized mean value and standard deviation for each were calculated and plotted in the graph using Prism 7 software and the statistical significance was calculated using a one-way Anova test.

4. Conclusions

The sensitivity and specificity of **NG1** towards Cu^{2+} ions are tested by various spectroscopic and biophysical assay. Finally, the supramolecular assembly of the probe was studied and it suggested that disaggregation mediated by Cu2+played crucial role in producing yellow fluorescence. Further, it was found that the yellow fluorescence is completely quenched on the addition of Lactic acid suggesting the application of **NG1** for sequential detection ofCu2+ and lactate. Since high levels of lactate ions and Cu^{2+} ions are associated with many pathological disorders, the results presented in the manuscript could be immense importance for the designing of a simple and cost-effective technique for dual detection of Cu^{2+} and lactate.

In addition to the experimental study, DFT calculations were also carried out various possible probes **NG1**, **NG2,** andNG**3** withCu^{2+} ions atom and lactic acid to support our experimentally observed results. The comparison of experimental and theoretical results reveals a good agreement between experimental findings and calculated results and shows the same pattern of shifting in absorption towards higher wavelength.

Funding sources

The work was supported by the DST SERB extramural research fund (Project No. EMR/2016/003186) received by Dr. Nidhi Gour and DST-SERB Ramanujan Fellowship to Dhiraj Bhatia.

Author contributions

NG proposed the application of probe while VK synthesized the probes NG1, NG2 and NG3. .UV, and Self-assembly, Fluorescence study was done by the BK and VK jointly. DS and …did DFT experiments SK and DB devised cell culture experiments. SK performed the Cellular uptake and quantification of dye uptake in cells. All the authors discussed the results and contributed tomanuscript drafting**.**

Acknowledgments

NG, VK, and CKP greatly acknowledge support from DST and SERB research grant (EMR/2016/003186) for funding and fellowships. BK thanks Indrashil university for funding and infrastructure support. DS thanks GSBTM for fellowship.We thank Central Imaging Facility (CIF) at IITGN for confocal microscopy and the initial seed funding from IITGN to Dhiraj

Bhatia. NG also greatfully acknowledge Prof Ehud Gazit (Tel Aviv Unviersity, Israel) and Dor zaguri for useful discussion and experimental support.

References

1. Valdez, C. E.; Smith, Q. A.; Nechay, M. R.; Alexandrova, A. N. J. A. o. c. r., Mysteries of metals in metalloenzymes. **2014,***47* (10), 3110-3117.
2. Mocchegiani, E.; Costarelli, L.; Giacconi, R.; Piacenza, F.; Basso, A.; Malavolta, M. J. A. r. r., Micronutrient (Zn, Cu, Fe)–gene interactions in ageing and inflammatory age-related diseases: implications for treatments. **2012,***11* (2), 297-319.
3. Osredkar, J.; Sustar, N. J. J. C. T. S., Copper and zinc, biological role and significance of copper/zinc imbalance. **2011,***3* (2161), 0495.
4. Bremner, I. J. T. A. j. o. c. n., Manifestations of copper excess. **1998,***67* (5), 1069S-1073S.
5. Fitzgerald, D. J. J. T. A. j. o. c. n., Safety guidelines for copper in water. **1998,***67* (5), 1098S-1102S.
6. Bakkaus, E.; Collins, R. N.; Morel, J.-L.; Gouget, B. J. J. o. C. A., Anion exchange liquid chromatography–inductively coupled plasma-mass spectrometry detection of the Co2+, Cu2+, Fe3+ and Ni2+ complexes of mugineic and deoxymugineic acid. **2006,***1129* (2), 208-215.
7. Shamspur, T.; Mostafavi, A.; Sheikhshoaie, I. J. J. o. A. I., Determination of copper in water and plant samples by flame atomic absorption spectrometry after preconcentration on octadecyl silica membrane disks modified with a recently synthesized Schiff's base. **2008,***91* (4), 865-870.
8. Ren, L.; Chong, J.; Loya, A.; Kang2, Q.; Stair, J.; Nan, L.; Ren, G. J. M. T., Determination of Cu2+ ions release rate from antimicrobial copper bearing stainless steel by joint analysis using ICP-OES and XPS. **2015,***30* (sup6), B86-B89.
9. Zhang, S.; Niu, Q.; Lan, L.; Li, T. J. S.; Chemical, A. B., Novel oligothiophene-phenylamine based Schiff base as a fluorescent chemosensor for the dual-channel detection of Hg2+ and Cu2+ with high sensitivity and selectivity. **2017,***240*, 793-800.
10. Kaur, P.; Kaur, M.; Singh, K. J. T., Ferrocene based chemosensor for Cu2+—A dual channel signaling system. **2011,***85* (2), 1050-1055.
11. Cui, Z.; Bu, W.; Fan, W.; Zhang, J.; Ni, D.; Liu, Y.; Wang, J.; Liu, J.; Yao, Z.; Shi, J. J. B., Sensitive imaging and effective capture of Cu2+: Towards highly efficient theranostics of Alzheimer's disease. **2016,***104*, 158-167.
12. Aguirre, P.; García-Beltrán, O.; Tapia, V.; Muñoz, Y.; Cassels, B. K.; Núñez, M. T. J. A. c. n., Neuroprotective effect of a new 7, 8-dihydroxycoumarin-based Fe2+/Cu2+ chelator in cell and animal models of Parkinson's disease. **2017,***8* (1), 178-185.
13. Shi, Y.; Wang, R.; Yuan, W.; Liu, Q.; Shi, M.; Feng, W.; Wu, Z.; Hu, K.; Li, F. J. A. a. m.; interfaces, Easy-to-Use Colorimetric Cyanine Probe for the Detection of Cu2+ in Wilson's Disease. **2018,***10* (24), 20377-20386.
14. Petrelli, F.; Cabiddu, M.; Coinu, A.; Borgonovo, K.; Ghilardi, M.; Lonati, V.; Barni, S. J. A. o., Prognostic role of lactate dehydrogenase in solid tumors: a systematic review and meta-analysis of 76 studies. **2015,***54* (7), 961-970.
15. Frisch, M.; Trucks, G.; Schlegel, H.; Scuseria, G.; Robb, M.; Cheeseman, J.; Scalmani, G.; Barone, V.; Petersson, G.; Nakatsuji, H. J. G. S. T. i. n. c. r. f. t. r., Gaussian16, revision B. 01; Gaussian, Inc: Wallingford, CT, 2016. **2019**.
16. Khairul, W. M.; Zuki, H. M.; Hasan, M. F. A.; Daud, A. I. J. P. C., Pyridine Acyl Thiourea as Ionophore for the Detection of Copper (II) in Aqueous Phase. **2016,***20*, 105-114.
17. Hamedan, N.; Hasan, S.; Zaki, H.; Alias, N. In *Colorimetric chemosensor of symmetrical benzoylthiourea derivatives as for detection of Cu2+ in aqueous solution*, IOP Conference Series: Materials Science and Engineering, IOP Publishing: 2017; p 012038.
18. Hasan, S.; Hamedan, N. A.; Zaki, H. M. J. I. J. C. E. A., Application of P-dimethylaminobenzaldehyde benzoylthiourea as a colorimetric chemosensor for detection of Cu2+ in aqueous solution. **2017,***8* (1), 22.
19. Bharti, A.; Bharati, P.; Dulare, R.; Bharty, M.; Singh, D. K.; Singh, N. J. P., Studies on phenylmercury (II) complexes of nitrogen–sulfur ligands: Synthesis, spectral, structural characterization, TD-DFT and photoluminescent properties. **2013,***65*, 170-180.
20. Khandelwal, P.; Singh, D. K.; Sadhu, S.; Poddar, P. J. N., Study of the nucleation and growth of antibiotic labeled Au NPs and blue luminescent Au 8 quantum clusters for Hg 2+ ion sensing, cellular imaging and antibacterial applications. **2015,***7* (47), 19985-20002.
21. Majumdar, D.; Dey, S.; Das, D.; Singh, D. K.; Das, S.; Bankura, K.; Mishra, D. J. J. o. M. S., Heterometallic Zn (II)-K (I) complex with salen-type Schiff-base ligand: Synthesis, crystal structure, solid-state photoluminescent property and theoretical study. **2019,***1185*, 112-120.
22. Sanchora, P.; Pandey, D. K.; Rana, D.; Materny, A.; Singh, D. K. J. T. J. o. P. C. A., Impact of size and electronegativity of halide anions on hydrogen bonds and properties of 1-Ethyl-3-methylimidazolium-based ionic liquids. **2019,***123* (23), 4948-4963.
23. McAllister, M. A. J. J. o. M. S. T., Characterization of low-barrier hydrogen bonds 2. HF2−: a